

1 Auxiliary material for
2 “The spectral dimension of longwave feedbacks in the CMIP3 and CMIP5 experiments”
3 Xianglei Huang, Xiuhong Chen (University of Michigan), Brian J. Soden (University of
4 Miami), and Xu Liu (NASA Langley research center)
5 Geophysical Research Letters, 2014

6 **Introduction**

7 This auxiliary file contains five sections. Section 1 describes the technical details on
8 constructing the spectral radiative kernel. Section 2 contains figures and tabulated
9 broadband feedback strengths computed using both spectral kernel technique and
10 published broadband kernel techniques. Section 3 summarizes the basic information of
11 the CMIP3 and CMIP5 models used in this analysis. Section 4 is a plot for clear-sky
12 feedbacks in parallel to the all-sky feedbacks shown as Figure 3 in the text. Section 5
13 shows the all-sky lapse-rate feedbacks of two GCMs that have identical broadband lapse-
14 rate feedback strength.

15 **1. Technical details on constructing the SRK (spectral radiative kernels)**

16 Similar to the broadband radiative kernel technique [Soden and Held, 2006;
17 Soden *et al.*, 2008; Shell *et al.*, 2008], the LW TOA spectral flux change ΔR_X in response
18 to a change of non-cloud variable X at a frequency ν and over a latitude-longitude grid
19 (x, y) that is caused by an increase of surface temperature can be approximated as

20
$$\Delta \bar{R}_X(x, y; \nu) = \sum_{j=1}^N \left[\overline{\frac{\partial R(x, y; t; \nu)}{\partial X_j}} \cdot \overline{\Delta X_j(x, y; t)} \right] \quad (\text{S1})$$

21 where ΔX denotes response of variable X to surface temperature change. N is the number
 22 of vertical levels and j denotes the j -th level. The over-bar denotes monthly average.

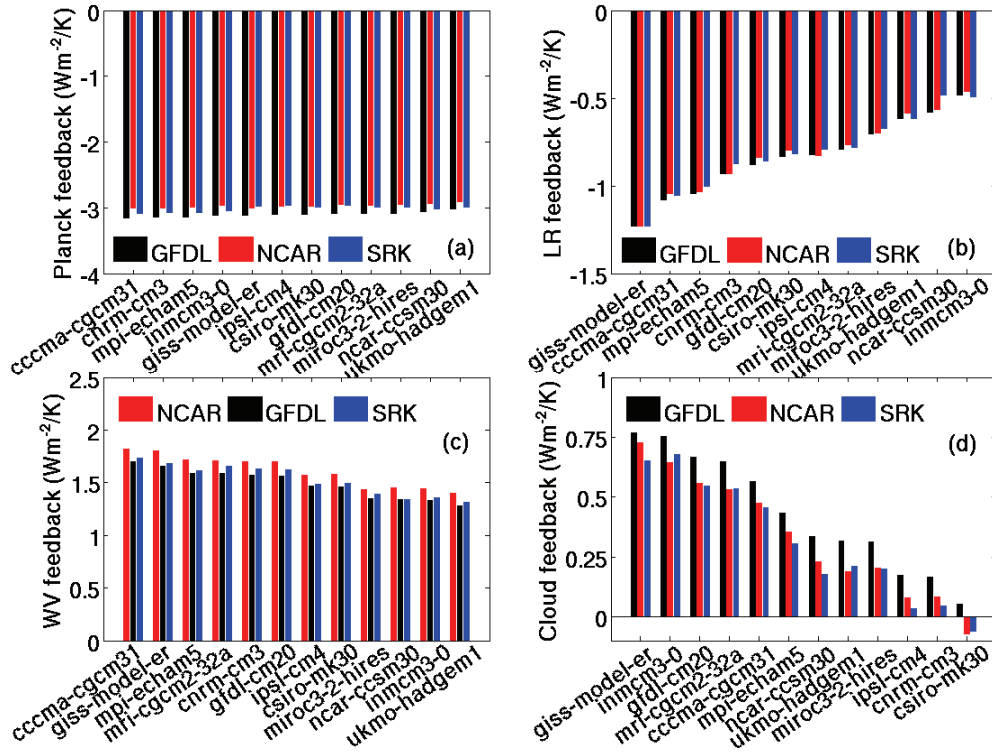
23 $\overline{\frac{\partial R(x, y; t; \nu)}{\partial X_j}}$ is the monthly-averaged SRK. It is derived from

$$24 \quad \begin{aligned} & \overline{\frac{\partial R(x, y; t; \nu)}{\partial X_j}} \\ & \approx \frac{R(X_1, X_2, \dots, X_j + \Delta X_j, \dots, X_N; x, y; t; \nu) - R(X_1, X_2, \dots, X_j, \dots, X_N; x, y; t; \nu)}{\Delta X_j} \end{aligned} \quad (\text{S2})$$

25 where the monthly average is computed using 3-hourly simulation output from the GFDL
 26 AM2 model, ΔX_j is a small perturbation of change in variable X_j . For water vapor, the
 27 natural logarithms of specific humidity (q) is used instead of q itself because, at the
 28 spectral width of our interest (i.e. 10cm^{-1}), small change in the TOA spectral flux is more
 29 linearly proportional to $\log(q)$ instead of q .

30 The GFDL AM2 model has a horizontal resolution of 2° latitude $\times 2.5^\circ$ longitude
 31 and 24 layers in vertical with top at 3 hPa. Specifically, the 3-hourly profiles of simulated
 32 temperature, specific humidity, cloud fraction, cloud liquid water content and cloud ice
 33 water content are fed into the PCRTM-based spectral flux simulator developed by *Chen*
 34 *et al.* [2013] to compute spectral flux at 10cm^{-1} interval for the entire LW spectral region.
 35 Instead of doing numerical perturbation as in *Soden et al.* [2008] and *Shell et al.* [2008] to
 36 obtain the Jacobians defined in Equation S2, the PCRTM can compute all the Jacobians
 37 simultaneously with the calculation of spectral flux, which greatly saves the
 38 computational cost. To use the SRKs for the feedback calculation, we multiply it with the
 39 monthly-mean difference in X for each calendar month and then sum over all 12 months
 40 to obtain the feedbacks as discussed in the text.

41 **2. LW broadband feedback strengths computed by different techniques**



42
43 Figure S1. (a) The longwave broadband Planck feedback strengths as computed using the
44 GFDL broadband radiative kernel (black bars), the NCAR broadband radiative kernel
45 (red bars), and the SRK method (blue bars), respectively. (b)-(d) Same as (a) but for the
46 lapse-rate, LW water vapor, and LW cloud feedback, respectively. The GCMs on each
47 panel is arranged according to the descending order of the individual feedback strengths
48 computed using the GFDL broadband radiative kernel.

49 Table S1. LW broadband feedbacks as computed by the GFDL radiative kernel (Soden et
50 al., 2008), NCAR radiative kernel (Shell et al, 2008, numbers in parentheses), and the
51 SRK developed in this study. LR, WV, and CL refer to lapse rate, LW water vapor, and
52 LW cloud radiative feedbacks, respectively. All feedbacks are computed by using the
53 kernels from surface to the tropopause. All results are expressed in units of $\text{Wm}^{-2} \text{ K}^{-1}$.
54 GCMs from the CMIP3 archives are used and the multi-model means are listed as well.

55 Simulations of the A1B scenario are used in all calculations. Further information of each
 56 model can be found below.

GCMs	Feedbacks computed using the LW broadband kernels of GFDL and NCAR (in parentheses) in $\text{Wm}^{-2} \text{K}^{-1}$				Feedbacks computed using the SRK in $\text{Wm}^{-2} \text{K}^{-1}$			
	Planck	LR	WV	CL	Planck	LR	WV	CL
ccma_cgcm3_1	-3.17 (-3.02)	-1.09 (-1.05)	1.70 (1.82)	0.57 (0.48)	-3.10	-1.06	1.74	0.45
cnrm_cm3	-3.15 (-3.01)	-0.93 (-0.93)	1.57 (1.70)	0.16 (0.08)	-3.09	-0.88	1.64	0.05
csiro_mk3_0	-3.12 (-3.00)	-0.84 (-0.80)	1.46 (1.58)	0.05 (-0.08)	-3.01	-0.82	1.50	-0.06
gfdl cm2.0	-3.10 (-2.97)	-0.88 (-0.84)	1.57 (1.7)	0.67 (0.56)	-2.97	-0.86	1.62	0.55
giss_model_e_r	-3.13 (-3.01)	-1.24 (-1.24)	1.66 (1.81)	0.77 (0.73)	-2.99	-1.24	1.69	0.65
inmcm3_0	-3.13 (-2.98)	-0.49 (-0.47)	1.33 (1.45)	0.75 (0.64)	-3.06	-0.50	1.36	0.68
ipsl-cm4	-3.12 (-3.00)	-0.83 (-0.83)	1.47 (1.57)	0.17 (0.08)	-2.97	-0.79	1.49	0.04
miroc3.2_hires	-3.09 (-2.96)	-0.71 (-0.70)	1.35 (1.44)	0.31 (0.20)	-3.01	-0.68	1.39	0.20
mpi-echam5	-3.15 (-2.99)	-1.05 (-1.04)	1.59 (1.72)	0.43 (0.35)	-3.08	-1.01	1.62	0.31
mri-cgcm2.3.2	-3.10 (-2.98)	-0.80 (-0.77)	1.59 (1.71)	0.64 (0.53)	-3.00	-0.78	1.66	0.53
ncar_ccsm3_0	-3.08 (-2.96)	-0.58 (-0.57)	1.34 (1.45)	0.33 (0.23)	-3.03	-0.49	1.34	0.18
ukmo_hadgem1	-3.04 (-2.91)	-0.62 (-0.59)	1.28 (1.40)	0.31 (0.19)	-3.00	-0.62	1.32	0.21
Multi-model mean	-3.11 (-2.98)	-0.84 (-0.82)	1.49 (1.61)	0.43 (0.33)	-3.02	-0.81	1.53	0.32

57
 58

59 3. Name lists of GCMs used in the analysis

60 Below is a list of the 12 pairs of GCMs used in this study and their sponsors, as
 61 well as the horizontal resolutions of each GCMs. As in the text, the CMIP3 model names
 62 are in lower case and the CMIP5 ones in upper case.

Model name (Horizontal resolution)		Sponsor(s), Country
CMIP3 in 1pctto2x	CMIP5 in 1pctco2	
ccma_cgcm3_1 (~2.8°×2.8°)	CanESM2 (~2.8°×2.8°)	Canadian Center for Climate Modelling and Analysis, Canada
cnrm_cm3 (~1.9°×1.9°)	CNRM-CM5 (~1.4°×1.4°)	Centre National de Recherches Météorologiques, France
csiro_mk3_0 (~1.9°×1.9°)	CSIRO-Mk3-6-0 (~1.9°×1.9°)	The Commonwealth Scientific and Industrial Research Organization, Australia
gfdl_cm20 (2°×2.5°)	GFDL-CM3 (2°×2.5°)	Geophysical Fluid Dynamics Laboratory, USA
giiss_model_e_r (4°×5°)	GISS-E2-R (2°×2.5°)	NASA/GISS, USA
inmcm3_0 (4°×5°)	INMCM4 (1.5°×2°)	Russian Institute for Numerical Mathematics, Russia
ipsl_cm4 (2.5°×3.75°)	IPSL-CM5A-LR (1.9°×3.75°)	Institute Pierre Simon Laplace, France
miroc3_2_hires (1.125°×1.125°)	MIROC5 (1.4°×1.4°)	Atmosphere and Ocean Research Institute (The University of Tokyo), Japan
mpi_echam5 (1.875°×1.875°)	MPI-ESM-LR (1.875°×1.875°)	Max Planck Institute for Meteorology, Germany
mri_cgcm2_3_2a (~2.8°×2.8°)	MRI-CGCM3 (~1.125°×1.125°)	Meteorological Research Institute, Japan
ncar_ccsm3_0 (1.41°×1.41°)	CCSM4 (0.9°×1.25°)	National Center for Atmospheric Research, USA
ukmo_hadgem1 (~1.3°×1.9°)	HadGEM2-ES (~1.3°×1.9°)	UK Met Office Hadley Centre, UK

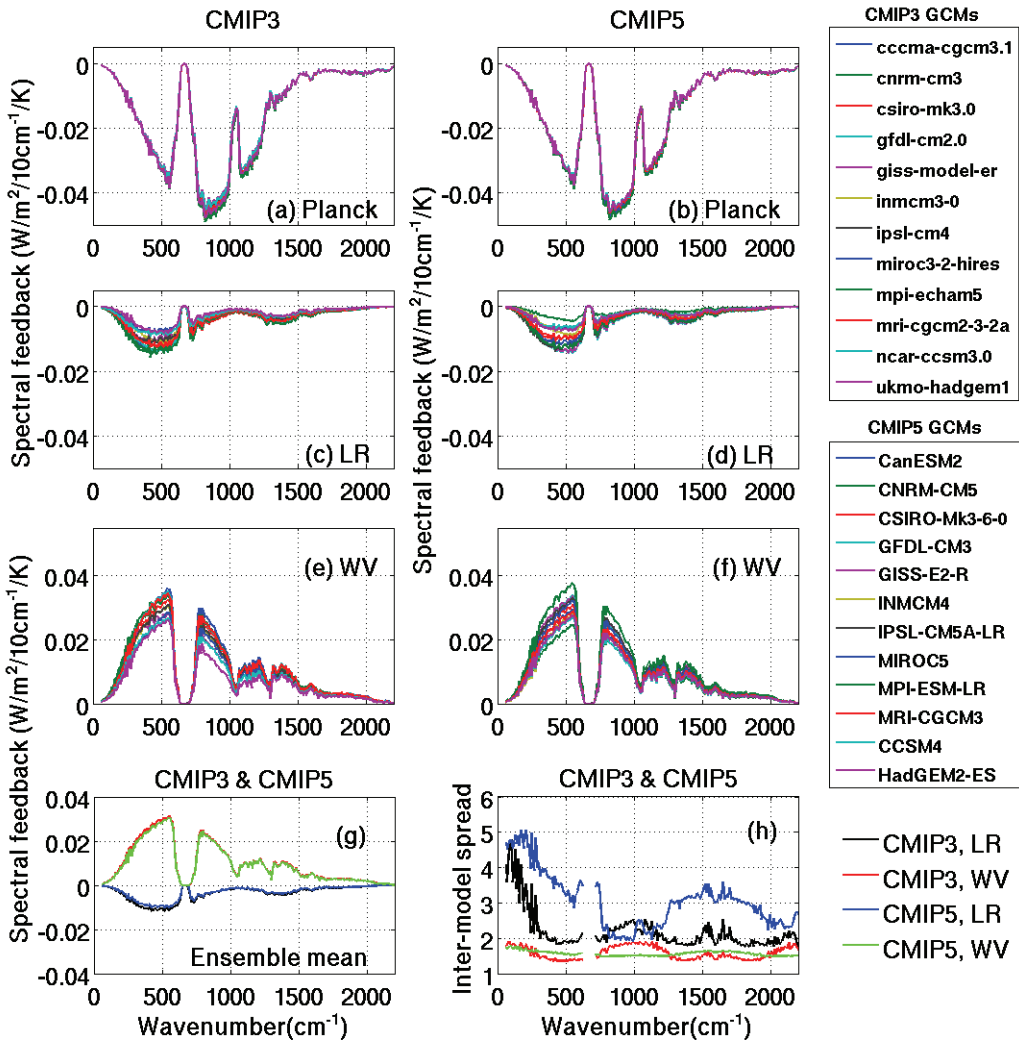
63

64

65

66

4. Clear-sky spectral feedback from CMIP3 and CMIP5

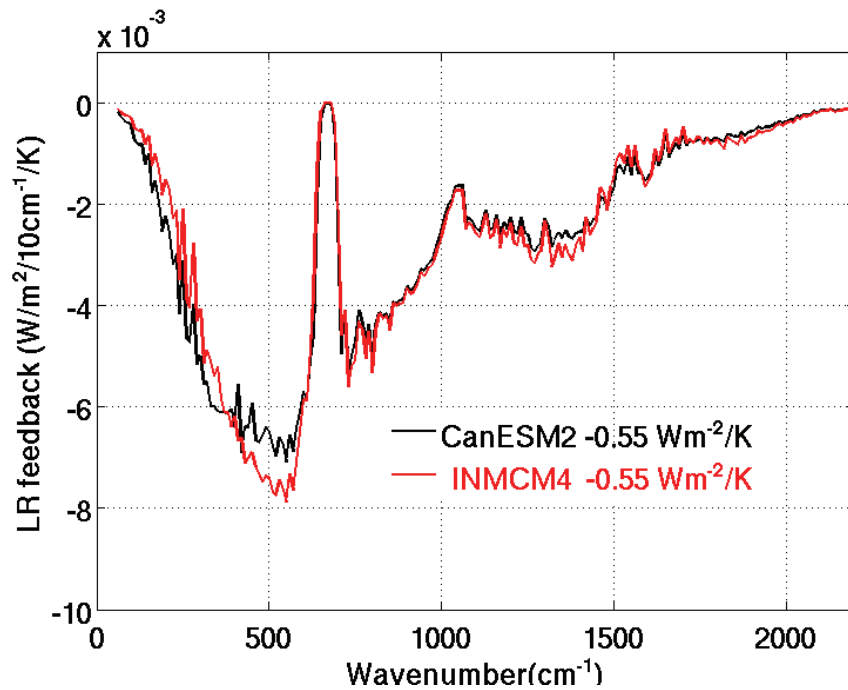


67
68

69 Figure S2. Same as Figure 3, but for clear-sky LW spectral feedbacks. As shown
70 by the figure, virtually all features discussed in the text regarding all-sky LW spectral
71 also exist in the clear-sky LW spectral feedbacks.

72
73 **5. Spectral lapse-rate feedbacks of CanESM2 and INMCM4**

74



75

Figure S3. The all-sky spectral lapse rate feedbacks of CanESM2 and INMCM4. Though
76 two GCMs have identical broadband lapse-rate feedback strength, the compensating
77 differences in far-IR is obvious.